New regional stratigraphic insights from a 3D geological model of the Nasia Sub-basin, Ghana, developed for hydrogeological purposes and based on reprocessed B-field data, originally collected for mineral exploration

5   Elikplim Abla Dzikunoo[1], Giulio Vignoli[2,3], Flemming Jørgensen[4], Sandow Mark Yidana[1] and Bruce Banoeng-Yakubo[1]

[1]Department of Earth Science, University of Ghana, Accra, Ghana

[2]DICAAR, University of Cagliari, Cagliari, Italy

[3]GRUK, Geological Survey of Denmark and Greenland (GEUS), Aarhus, Denmark

10   [4]Central Denmark Region, Viborg, Denmark

Correspondence to: Sandow Mark Yidana (yidanas117@gmail.com) and Elikplim Abla Dzikunoo (eadzikunoo@gmail.com)

Abstract. Re-processing of regional-scale airborne electromagnetic data is used in building a 3D geological model of the

15   Nasia Sub-Basin, Northern Ghana. The resulting 3D geological model consistently integrates all the pieces of information brought by the electromagnetic data, lithologic logs, ground-based geophysical surveys and the prior geological knowledge of the terrain based on previous research. The geo-modelling process is aimed at defining the lithostratigraphy of the area, chiefly to improve the stratigraphic definition of the area as well as for hydrogeological purposes. The airborne electromagnetic measurements, consisting of GEOTEM B-field data, were originally collected for mineral exploration

20   purposes. Thus, those B-field data had to be (re)processed and properly inverted as the original survey and data handling were designed for the detection of potential mineral targets and not for detailed geological mapping. These new geophysical inversion results, compared with the original Conductivity Depth Images, provided a significantly different picture of the subsurface. The new geophysical model led to new interpretations of the geological settings and to the construction of a comprehensive 3D geomodel of the basin. In this respect, the evidences of a hitherto unexposed paleovalley could be

25   inferred from the airborne data. The stratigraphic position of these paleovalleys suggests a distinctly different glaciation history from the Marinoan events, commonly associated with the Kodjari formation of the Voltaian sedimentary basin. Indeed, their presence may be correlated to mountain glaciation within the Sturtian period though no unequivocal glaciogenic strata have yet been identified. This pre-Marinoan glaciation is recorded in rocks of the Wassangara group of the Taoudeni basin. The combination of the Marinoan and, possibly, Sturtian glaciation episodes, both of the Cryogenian period,

30   can be an indication of a Neoproterozoic Snowball Earth. Hence, the occurrence of those geological features, do not only have an important socio-economic consequences - as the paleovalleys can act as reservoirs for groundwater - but, also from a

scientific point of view, could be extremely relevant - as their presence would require a revision of the present stratigraphy of the area.

1 INTRODUCTION

35   The present research demonstrates the effectiveness of reprocessing and proper inversion of existing airborne electromagnetic (AEM) data - more specifically, GEOTEM B-field measurements - for data-driven inference of the subsurface geology. More specifically, the AEM results are employed to develop a 3D geological model for subsequent hydrogeological conceptualization, and scenario simulations in the partially metamorphosed sedimentary Nasia sub-catchment of the White Volta Basin in Northern Ghana. In fact, the overall objective of the research is to develop a

40   decision-support tool for understanding groundwater occurrence to facilitate efficient development and optimization of the water resources in the basin within the framework of the GhanAqua project (funded by DANIDA). The geological interpretation of the newly reprocessed AEM data has highlighted potential evidences of paleovalleys, which, in turn, might have great socio-economic and scientific impacts. Indeed, such geological features could be possible groundwater reservoirs and lead to the revision of the current stratigraphy of the area.

45   The use of groundwater resources for crop irrigation offers an opportunity for a buffer against the unremitting impacts of climate change in Northern Ghana, where peasant farming is the mainstay of livelihood. The development of groundwater resources to support irrigation endeavours is particularly important because of erratic rainfall patterns during the rainy season and high temperatures and evapotranspiration rates in the dry season, which render surface water resources unsustainable reservoirs of irrigation water (Eguavoen, 2008). Erratic rainfall patterns in the region in recent times have affected crop

50   production and sustainable livelihoods of communities. Hence, improved access to groundwater resources for all year-round irrigation would boost agricultural development and offer increased employment possibilities in the area. However, over the years, access to sustainable groundwater resources has been hampered by the lack of sufficient knowledge of the local geological and structural geological setting. Such knowledge is crucial to the understanding of the hydrogeology and groundwater storage conditions and would be crucial for sustainable resource development.

55   Generally, the difficulty in defining and effectively characterizing subsurface geological conditions in an area such as the Voltaian hinges on the unavailability of enough reliable data (e.g., lithological logs of deep boreholes) and the limitations inherent in conventional ground-based geophysical techniques (e.g., poor spatial coverage and insufficient density). So, a multi-scale, holistic approach, integrating the airborne geophysical insights with all the available lithological borehole logs and, former and present, ground-based geological investigations is showed to be essential for the development of an effective

60   and coherent geological model to be eventually used for hydrogeological scenario assessments.

  Three-dimensional (3D) geological modelling based on specifically collected AEM data for hydrogeological applications is, in general, not new (Jørgensen, Møller, et al. 2013; Jørgensen, et al. 2015; Høyer, et al. 2015; Oldenborger, et al., 2014), but as far as we are concerned, it has never been done before using B-field measurements. Additionally geological modelling for

hydrogeological application is novel in the West African sub-region, even though the region has a rich database of pre-
existing AEM data from former mineral exploration surveys. Hence, the application of the presented workflow for inversion
of AEM data can potentially be extended to many areas in this part of the African continent, and, in general, everywhere pre-
existing AEM data is available. This can help avoid the costs connected with the airborne data collection: which is often
considered affordable for mineral exploration, but prohibitive for groundwater mapping.

In addition, the geological interpretation of the newly reprocessed AEM data (with their significantly enhanced information
content) facilitated the discovery of evidence showing the presence of potential paleovalleys, possibly acting as groundwater
reservoirs. At the same time, the existence of such geological features and, in particular, their stratigraphic location within
the Panabako formation suggests the need for a possible revision of the stratigraphy of the Bombouaka group, especially
within the study area. Additionally, the new insights suggest that there was some pre-Marinoan glacial activity (Hoffman and
Li, 2009) in the Voltaian sedimentary; preceding the Marinoan glaciation episode, generally associated with the Kodjari
formation of the basin (Deynoux et al. 2006) both within the Cryogenian period. This new glaciation suggests that the
possibility of a Sturtian event, but this assertion is currently hypothetical and would need further investigations to verify. The
proposed combination of the Marinoan and Sturtian events in the Neoproterozoic Voltaian sedimentary basin, if verified
would be compatible with the hypothesis of a global Neoproterozoic Snowball Earth even in low latitude areas (Bechstädt et
al., 2018; Hoffman and Schrag 2002).

2 DATA AND METHODS

2.1 The Study Area

The approximately 5,300 km^2 area of the Nasia Basin is found in the Northern Region of Ghana, within the Guinea
Savannah belt. It is associated with an average annual rainfall of 1000-1300 mm, which peaks between late August and early
September. Torrential rains within this peak season create serious drainage problems as the infiltration rates are low due to
the largely impervious nature of the various lithologies, creating high amounts of runoff, in turn, leading to high levels of
erosion and posing significant constraints on agriculture (FAO, n.d.).

The area is characterized by relatively low relief in the south, and a few areas of high elevation associated with the Gambaga
escarpment to the north. The basin drains a left bank tributary of the White Volta, the Nasia River (Fig. 1a) and is underlain
by sedimentary rocks of the Bombouaka and Oti-Pendjari groups of the Neoproterozoic Voltaian Supergroup, and comprised
predominantly of variations of sandstones, siltstones and mudstones (Carney et al., 2010). Detailed descriptions of the
geologic units can be found in Carney et al., (2010) and, also in Jordan et al. (2009).

2.2 Data and Modelling Requirements

A 3D geomodel of an area is a synthesis of all relevant geologic information available; during the construction process, it is
essential to integrate and merge multiple data sources and scales in order to appropriately represent the different aspects of a

95 complex geologic systems (e.g., Dzikunoo et al. 2018; Rapiti et al, 2018; Jørgensen et al., 2015; Vignoli et al., 2017; Høyer et al. 2017; Vignoli et al, 2012). In this regard, the diverse kinds of data used in this study consist of: i) AEM data (namely, GEOTEM B-field), ii) borehole lithological and geophysical logs, and iii) ground-based Electrical Resistivity Tomography (ERT).

An important underlying consideration for the construction of a lithostratigraphic model is the definition of a conceptual

100 model initially developed from the prior knowledge of the terrain (Fig. 1b). Interpretations from geophysical signatures are then tied into the conceptual model followed by the development of a model framework with interpretation points and, subsequently, populated with voxels, each characterized by homogeneous attributes. Clearly, any piece of information brought, in this specific case, from the geophysics can/must be used, via a confirmation/rejection process, to refine the initial geological hypotheses (Tarantola, 2006).

105 **2.2.1 Airborne Electromagnetic Data (AEM)**

A fixed-wing Casa 212 aircraft, equipped with a 20-channel GEOTEM multi-coil system, was used to acquire the time-domain electromagnetic data (Fugro Airborne Surveys, 2009a,b) with both a line spacing of 20 km (flown at 042° - 132° along and across the general geologic strike lines within the Volta Basin) and a much denser line spacing of 200 m (flown at 000° - 180°). The locations of the flight lines of both surveys (dense and regional) are shown as red lines in Fig. 1a (the 200

110 m spacing makes the dense survey appear almost as a red rectangle). The GEOTEM surveys were performed under the auspices of the European Union Mining Sector Support Programme 2005 to 2008 and were designed for mineral exploration. Within the present study, the original B-field data have been reprocessed and inverted; this is to ensure the preservation of all the corrections applied to the raw data by Fugro, and, contextually, to have the opportunity to consistently compare the new outcomes with the Conductivity Depth Images (CDIs) provided by the survey company as final deliverables (Fugro Airborne

115 Surveys, 2009a,b). This comparison was necessary in order to estimate what could be gained by going through a complete reprocessing and inversion round in terms of reliability and accuracy of the subsequent (hydro) geological model(s). Since the data acquisition was originally focused on mineral targeting, the specifications of the survey, and, also, the choice of CDIs as deliverables, were intended to optimize the detection, even at depth, of large conductivity contrast targets (typical for mineral exploration) with, potentially, a high lateral resolution. Conversely, for geological mapping purposes, the

120 capability to retrieve, via proper inversion strategies, even low-contrast conductivity features and, at the same time, to reproduce the spatial coherence of the geological features is crucial. Therefore, it was important to double-check the effectiveness of the new inversion approaches and of the dedicated preliminary data conditioning.

In addition, as discussed in Smith and Annan, 1998, the choice of B-field has some further advantages in terms of noise-signal ratio as the B-field is associated with data integration over time that can act as some sort of stacking in time. Clearly,

125 the data stacking can (should) be performed also in the other "direction", that is, spatially, along the line of flight. In the workflow implemented in this research, the optimal lateral time-dependent stacking window was selected by checking gate-

by-gate the minimum width capable of preserving the spatial variability visible in the data, but, also, of reducing erratic oscillation of the signal.

With respect to the inversion, as the receiver of the GEOTEM system is located in a towed-bird, altitude, pitch and roll of the device were part of the inversion parameters, and they were reconstructed by using the Z and X components of the B-field measurements and by enforcing a lateral continuity between adjacent measurement locations. Similar approach has been used also for the main model parameter we inverted for the electrical resistivity. So, in the framework of a pseudo-3D inversion based on a 1D forward modelling, the resistivity of a specific discretizing layer was coupled to the resistivity values at the corresponding depths in the closest 1D soundings. Thus, for the data collected with a 200 m line spacing, we applied the so called Spatially Constrained Inversion (SCI – Viezzoli et al, 2008), while for the less dense acquisition data (20 km line spacing), its 2D version (Laterally Constrained Inversion - LCI) was used instead. The final results clearly depended on the specific choices of the inversion settings (e.g. the relative weight of the regularizing term connecting the resistivities of layers of different soundings) and the choices of the inversion strategy (e.g. sharp versus smooth regularization – Auken et al., 2014; Ley-Cooper et al. 2014; Vignoli et al., 2015; Vignoli et al., 2017). In order to select the most effective regularization capable of retrieving a resistivity distribution compatible with: i) the observations within the noise level, and ii) the most reasonable geological expectation, we adopted an iterative geophysics-geology approach, characterized by a close interaction between geologists and geophysicist. The basic rationale behind this is that the geological interpretation already starts at the geophysical processing stages. For the large majority of the Nasia sub-catchment, a smooth regularization has been used with extremely loose (compared with those generally used for the standard dB/dt-data inversion – e.g., Viezzoli et al. 2010 and Viezzoli et al. 2013) lateral and vertical constraints. The result is a quasi-3D resistivity volume generated from B-field GEOTEM data that is significantly different (in terms of possible geological interpretation) from the original CDIs (Fig.2).

2.2.2 Electrical Resistivity Tomography

2D ERT surveys were performed at different locations in order to optimally site new boreholes and to investigate the nature of the near subsurface within the study area. Figure 1a shows the locations of the DWVP wells which were sited using ERT. ERT lines were extended to either 400 m or 800 m with electrode spacing of 20 m.

The observed apparent resistivities have been processed to remove evident spurious data points, and, subsequently, inverted using RES2DINV (Meier, et al., 2014; Loke, 1997; Loke and Barker, 1996) (Fig. 4).

2.3 3D Geo-modelling Procedure

2.3.1 Bedrock Geology

Raw data collected from various sources can be interpreted in terms of spatial variations (providing information about the geometries) and/or in terms of the absolute value of the attribute retrieved from the data (characterizing not only the geometry of the features, but also their nature).

The spatial information was used to create a 3D geometry model. Geometric modelling involves two steps. The first concerns the development of a suitable geometric representation of the fundamental geological "framework"; the second relates to the discretization of this framework to provide control for the analytical computations within the numerical models used in the predictive modelling (Turner, 2006).

In the present research, the first stage in the geometric modelling involved the interpolation of inverted 1D AEM data (Fig. 3) into a 3D grid with an assigned search radius of 20 km and a cell size of 2 km, for the regional data, and a search radius of 500 m and a cell size of 100 m, for the dense area. The assigned search radius should be not be less than the spacing between flight lines, to obtain continuous electrical resistivity distribution (Pryet et al., 2011), but, at the same time, it needs to be small enough to prevent smearing of possible useful information. The second, more laborious, step involved constructing the surfaces which define the overall units. Here, both the AEM and borehole data were correlated to a particular stratigraphic unit and the boundaries for that unit were drawn. This is necessary, and very tricky, since the electrical resistivity as it is inferred from the AEM cannot be unambiguously made to correspond to a specific lithology/stratigraphic unit. Clearly, for this task, not only the knowledge of the geophysical response behaviour, but, clearly, also the experience of the geologists in outlining which signatures belong to which stratigraphic unit, are equally crucial. For instance, low resistivity signatures within the Bombouaka may belong to the Poubogou formation, whereas anomalies with similar low resistivity ranges within the Oti may belong to the Bimbila formation. Also for this reason, the tight interaction between geologists and geophysicists (through several iterations) has been found crucial for an effective geomodelling.

Thus, the geomodelling can be considered as a way to compile, in a consistent manner, the geological knowledge about the area, the information from the dense geophysics (which acts as a "smart" interpolator between the available boreholes) and the other ancillary data. In this respect, it is worthwhile to note that only boreholes which had a distance smaller than 1-3 km from the flight lines were considered sufficiently representative for the geophysical interpretation.

The outlined boundaries were, then, used, in the next stage, for populating the model grid (Ross et al., 2005; Sapia, et al., 2015; Jørgensen, et al., 2013). Populating the model grid is done by adding and editing voxel groups based on a cognitive approach (Fig. 5 - Høyer, et al., 2017; Høyer, et al., 2015; Jørgensen, et al., 2013).

2.3.2 Regolith

The AEM data does not have the sufficient shallow resolution to effectively investigate the regolith layers that, however, are fundamental to understand the shallow groundwater behaviour. It is also for this reason that ERT data were collected and

used to infer the weathered zone. The regolith depths were derived from borehole logs and ERT interpretations, and gridded to form a basal surface, referred to as the bedrock surface in Gulbrandsen et al. (2018). Outlines of the regolith, as they can be found in Geological Survey Department (2006), were used as constraints, together with the terrain and the regolith depth grids, to create the 3D interpolation (Fig. 6a).

190   The obtained 3D regolith grid was then merged with the 3D bedrock grid to offer a complete picture of the subsurface geology (Fig. 6b).

3 RESULTS AND DISCUSSIONS

3.1 Inverted AEM data

Figure 2 shows an example of the comparisons between the original CDIs and the new inversion obtained with the discussed

195   SCI approach applied on the B-field GEOTEM data. The differences are evident. Not surprisingly, the CDI result is characterized by higher lateral variability, as each sounding is converted into a resistivity profile independently, while the SCI, by definition, enforces some degree of spatial coherence. The more prominent CDI's lateral heterogeneity is clear not only, on the N-E side of Fig. 2a, in the shallow portion of the section, where well-distinct resistive inclusions are detected, but also, at depth, along all the flight lines where there are spurious lateral oscillations of the electrical properties. The SCI

200   result is laterally more consistent; however this does not prevent the reconstruction of a resistive body, at a distance of approximately 10 km, that is well-separated from the resistive superficial unit - continuing on the right - by a clear conductive formation (very differently from what is retrieved by the CDI). In addition, the SCI result shows interesting resistive features incised into the more conductive surroundings (in particular, cfr. the two deepening structures located between 20 and 30 km). It is worth noting the considerable depth of investigation (DOI - indicated as a white mask in

205   Fig.2b); generally, the geophysical model parameters can be considered sensitive to the data down to the considerable depth of ~500 m. This, not only, demonstrates the quality of the original data, but, also, confirms that the survey was designed for deep exploration and not for high-resolution shallow investigations. Therefore, the new SCI provides important insights on the geological settings and highlights resistive, relatively shallow structures, possibly relevant as groundwater reservoirs.

In order to proceed further with the geological interpretation of the geophysical model, the SCI result was gridded (Fig. 3).

210   The general signature trends visible in such a resistivity grid can be summarized as follows:

•   areas with low resistivity values characterize argillaceous layers; in both the Bombouaka and Oti

•   sandstones have characteristically high resistivity values, with the massive quartzose sandstones of the Bombouaka and Kwaku Groups (specifically, the Panabako Sandstone, Anyaboni Sandstone, and upper Damongo Formation) displaying the lowest conductivities (Fugro Airborne Surveys Interpretation, 2009b).

3.2 Inverted ERT data

The difference in resistivities between fresh rocks and their weathered equivalents enable demarcation of the weathered zone. The example in Fig. 4 demonstrates the capability of electrical resistivity to outline the weathered zones. These geophysical observations are then compared against the available borehole data. Along this profile, three distinct layers are observed: i) the first one has high resistivities towards the southwest and decreasing values towards the northeast; ii) the second layer has low to moderate resistivities; and iii) the deepest is characterized again by high resistivities.

Considering the terrain, i.e. Panabako sandstones within which this profile was undertaken (Fig. 1a), it can be inferred that:

    i)   The first layer towards the southwest, which is approximately 10 m thick, with an average resistivity of 500 to more than 5000 Ohm·m, is the weathered zone which includes hardpan alternatively referred to as the saprolite and saprock. From the midpoint, towards the NE, resistivity signatures are similar to that of the underlying second layer.

    ii)   The second layer, which is approximately 30 m thick, can be considered to be part of the bedrock. Its characteristic low resistivity signature could be attributed to a fracture system (at the midpoint of the profile), confirmed by the evidences observed during drilling between the depths of 40 m to 50 m below the surface; the sandstones records resistivity values between 22 to 490 Ohm·m. Additionally, the profile is less than 5 km away (at both ends of the line) from regional E-W *(sensu lato)* brittle faults identified by Crowe & Jackson-Hicks (2008).

    iii)   The bedrock, which is made up of fresh feldspathic quartz rich arenites, records resistivity values between 500 and >5000 Ohm·m.

Figures 5 and 6 are images of, the geology and regolith, respectively, in the study area. They are mainly based on the geophysics (ERT, AEM) and the ancillary information (regolith outlines from previous radiometric survey - Geological Survey Department, 2006). The developed Nasia Basin geological model (Fig.s 5 and 6) consists of 17.5 million voxels, each with 500 m x 500 m lateral size and 5 m thickness. The model shows a coherent 3D representation of the subsurface within the Nasia Basin including the weathered zone. This generally honours the available geologic knowledge as well as the information from the wells, and the AEM evidences. Moreover, it provides some new insights into the geology of the terrain.

3.3 Lithostratigraphy from AEM

Figure 5 and 6 show nine distinct stratigraphic units in the study area. These include: i) Bunya (Youngest), ii) Bimbila +1, iii) Bimbila Shale, iv) Bimbila -1, v) Kodjari Formation, vi) Upper Panabako Sandstone, vii) Lower Panabako Sandstone, viii) Poubogou Formation and ix) Tossiegou Formation (Oldest).

3.3.1 The Bombouaka Group

In the study area, the Poubogou and Panabako formations of the Bombouaka Group outcrop in the north. On the contrary,
250 outcrops of the basal unit of this group, the Tossiegou Formation, have not been observed within the study area.

Tossiegou Formation

This is the oldest unit of the Bombouaka group. Rocks of this formation are not seen outcropping in the study area. However,
their signature is picked from the inverted AEM data as ranging approximately between 30 and 120 Ohm·m. The formation
255 is comprised of basal argillaceous strata which grade upwards into feldspathic and quartzitic sandstones (Carney, et al.,
2010). They overlie crystalline basement rocks of the Birimian (Anani et al., 2017). For example, from the NE-SW section
across the resistivity volume shown in Fig. 7, the Tossiegou formation is seen to extend way beyond 140 m below sea level.
An estimation of the thickness of the formation is however made difficult by its extension below the DOI. In fact, the great
depth of the formation, together with the overlying more conductive layers (the Bimbila and Poubogou formations),
260 generally, prevent the electromagnetic signal from propagating to greater depths making the inferred resistivity values of that
formation poorly sensitive to the data (and so, difficult to be resolved precisely).

Poubogou Formation

This unit is confined to the Gambaga escarpment with an average thickness of 170 m and grades upwards into the Panabako
265 formation with an increase in the arenaceous material (Fig. 7). The basin-wide distribution of this sequence indicates a
possible regional transgression event (Fugro Airborne Surveys Limited, 2009). The formation consists of green-grey,
micaceous mudstones and siltstones intercalated with sandstones at some places. As it grades into the overlying Panabako
formation, there is an increase in the sandstone proportion relative to the argillaceous beds (Carney et al., 2010). This
formation exhibits a poor resistive layer in AEM profiles ranging between 0 to 20 Ohm·m and appears to have a thicknesses
270 in the range of 150-180 m along a NE – SW profile in the study area. This is consistent with thicknesses recorded by Carney
et. al (2010).

Panabako Formation

This is a quartz-arenite rich formation with a suggested thickness of 150-200 m (Carney et al., 2010). Lithostratigraphic
275 mapping by Ayite et al. (2008) identified two subdivisions of the Panabako Formation within the Nakpanduri escarpment.
The upper division consists of near shore aeolean sequence, while the lower sequence is composed of near shore fluvial
sequence (lower Nakpanduri Sandstone formation); Carney et al. (2010) correlate the lower Nakpanduri to upper Poubogou.
From the current AEM data, this subdivision is however observed entirely within the Panabako with the presence of a

distinct resistivity contrast clearly visible in the newly inverted data (e.g. Fig. 7); indeed, in the new AEM reconstruction, the
upper Panabako shows higher resistivities - ranging from approximately 60 to 200 Ohm·m - and the lower layer is
characterized by relatively moderate conductivity - roughly between 30 and 60 Ohm·m. The tendency of the Bombouaka
Group sandstone units to fine towards argillaceous strata at their base (Jordan et al., 2009) can be inferred from the
increasing conductivity values towards the base, indicating a probable increase in argillaceous material.

3.3.2 The Oti Group

This group underlies the southern portion of the study area. Generally, it records the transition from a shallow marine
environment adjacent to a rifted margin into a marine foreland basin sequence represented by interbedded argillaceous and
immature arenaceous material (Carney et al., 2010).

Kodjari Formation

Composed of what is commonly known as the triad, this formation constitutes the basal unit of the Oti Group (Fig. 5).
Commonly, the Kodjari formation comprises: (i) basal tillites followed by, (ii) a cap-carbonate limestone, and finally
covered with (iii) laminated tuffs and ash rich siltstones (Carney et al., 2010).

The presence of the Kodjari formation is not easily seen, but can be inferred from the SCI resistivity sections by moderately
resistive strata observed immediately above the topmost units of the Bombouaka group (Fig. 7). An average thickness of 75
m can be retrieved; however, it should be noted that its continuity throughout the basin has not been verified. Carney et al.,
(2010) noted that, at some localities, in the north of the Volta Basin, the overlying tuffaceous material of the Kodjari triad is
seen to lie directly on the Panabako rocks of the Bombouaka as a result of the lateral discontinuity of these units. These
occurrences are confirmed also in the reprocessed AEM data (e.g. Fig. 7, at around 110 - 120 km).

Bimbila Formation

The Bimbila formation has two sandstone beds forming its upper and lower boundaries. These are the Chereponi Sandstone
member which form the basal stratum of the formation and the Bunya Sandstone member, which generates the exposed
upper portion of the formation. The Bunya sandstone is observed as a moderately conductive layer in the AEM cross section,
above the argillaceous material of the Bimbila (Fig. 7).

The argillaceous units of the formation consist mainly of green to khaki, micaceous laminated mudstones, siltstones and
sandstones representing a continuation of foreland basin deposition.

3.4 Structural Interpretations

The new results from the inversion of the AEM data reveal some amount of deformation within the basin. The arcuate nature of the basin, in addition to some other structures, is observed in the cross sections. Figures 7 and 8 show the generally curved

315 nature of the basin with dipping (approximately 20° from the surface) side slopes within the Bimbila.

Along line NE-SW 7 (Fig. 8), a vertical displacement is observed and is interpreted as a fault within the Bimbila. It aligns well (*sensu lato)* to late brittle faults (Crowe & Jackson-Hicks, 2008).

An angular conformity marking the transition between rocks of the >1000 Ma old Bombouaka rocks and the >600 Ma Oti rocks are observed in Fig. 7. The unconformity and the absence of sediments aged between 600 – 950 Ma could suggest the

320 presence of an oceanic gap which prevented the deposition of sediments (Kalsbeek et al., 2008).

The unconformity separates continental deposits of the Bombouaka below, from passive margin deposits of the Oti above (Kalsbeek et al., 2008).

Paleovalleys

325 Characteristic "U - shaped" valleys were interpreted from AEM data to the north of the basin (Fig. 7). The valleys exhibited a NW-SE trend and are considered to be tunnel valleys (Jørgensen & Sandersen, 2006; Kehew et al., 2012; Van der Vegt et al., 2012), the origin of which is still to be investigated. However, the presence of these valleys may be of stratigraphic interest as well as hydrogeologic significance.

The proposed presence of valleys between the Upper and Lower Panabako sequences represents an unconformity before the

330 deposition of the Upper Panabako sequence (Fig. 7). The geometry of the valleys, with their deep 'U' shaped nature, leads to the deduction that glaciation could play a role in their formation. Moreover, new insights into the stratigraphy may be implied with the possible presence of these valleys within the Panabako formation. The high energy event responsible for producing the intra-formational unconformity, most likely, occurred within the wide age range of ~1000 Ma to 635 Ma. The upper limit defined by the detrital zircon analysis of the Bombouaka group (Kalsbeek et al., 2008). Whereas, the lower

335 limits, representing the period of deposition of the tillites and diamictons of the Oti group within the Kodjari formation, should coorrespond to the end of the Cryogenian glacial period, which has been dated at 635 Ma (Carney, et al., 2010). This possible event would, however, be younger than 1100 Ma based on detrital zircon analysis. These valleys, then, represent a distinct history of glaciation separate from the Marinoan glaciation recorded in the Kodjari. This is similar to what is seen in the Wassangara group (Deynoux et al., 2006; Shields-Zhou et al., 2011) of the Taoudeni basin outcropping in western Mali

340 and southern Mauritania. Located in the southern region of the Taoudeni basin, thick successions of glacial influence have been recorded (Shields-Zhou et al., 2011) and were initially thought to form a part of Supergroup 2 of the Taoudeni basin. However, their presence below the craton wide erosional and angular unconformity marking the transition between Supergroup 1 and 2 precludes their association with the Marinoan glaciation of Supergroup 2 and includes them in what is

referred to as the Wassangara group rocks of Supergroup 1 (Deynoux, 2006; Shields-Zhou et al., 2011). Previous research
345   within the Voltaian, are replete with information on the glaciation within the Neoproterozoic Marinoan where an
unconformity between the top of the Bombouaka group and the basal units of the Oti-Pendjari group was proposed. This
unconformity is conspicuously marked by 'the Triad', consisting of basal tillites, cap carbonates and silicified tuffs
(Goddéris et al., 2003).

On the other hand, Deynoux et al., (2006) mention that the 400-500m thick glacially influenced succession was controlled by
350   the tectonic evolution of the nearby Pan-African belt with deposition at around 660 Ma. These proposed pre-Marinoan or
possibly Sturtian (~717 to 643 Ma) glacial events and deposits are suggested to be related to mountain glaciers (Bechstädt et
al. 2018; Deynoux et al. 2006; Villeneuve and Cornée 1994). Though these assertions are largely hypothetical, they are
feasible because of the low latitude position of the West African craton during the Proterozoic (Bechstädt et al. 2018;
Hoffman and Li 2009) combined with other geophysical and correlative (Dzikunoo et al., 2018; Shields-Zhou, et al. 2011)
355   evidence on the same craton.

The rocks of Bombouaka group in the Voltaian sedimentary basin are said to be reminiscent of the rocks in portions of
Supergroup 1 in the Taoudeni basin (Shields-Zhou et al., 2011) and the presence of glacial signatures in both groups
suggests that the pre-Marinoan glaciation must have been regional. The trends of the paleovalleys in the study area, i.e. NW-
SE align well to paleogeographic reconstructions of glaciation in NW Africa region which suggest the presence of an ice
360   sheet towards the north of the Reguibat shield with inferred glacial movement southwards towards the Pan-African belt
(Shields-Zhou et., 2011). The glacial movement is further verified by the transition of sediments in the region from glacial to
a mixture of glacial and marine and finally marine towards the border with the rocks of the Pan African belt. Some authors
consider that the combination of Sturtian and Marinoan glaciations - both of the Cryogenian - suggest a complete glaciation
event; i.e. the Snowball Earth where both continental and oceanic surfaces were covered by ice (Goddéris et al. 2003;
365   Hoffman and Li 2009; Macgabhann 2005).

The lack of pervasive evidence of the Sturtian glaciation within the Voltaian and the Taoudeni could be due to the
overprinting of glacial structures by the more recent Marinoan glaciation or tectonic activity related to regional subsidence
during the evolution of the Voltaian (Ayite, Awua, and Kalvig 2008).

Outcrop investigations of samples from the Bombouaka, however, do not show mixtites/diamictites which are typical of
370   glacial deposits and could either suggest a re-working of the glacial deposits by some fluvial action; this seems quite similar
to the situation Bechstädt et al. (2018) refers to as post-glacial transgression resulting in the infilling of incised valleys with
fluvial, reworked glacial and marine deposits. Carney et al (2010) observed two sandstone sequences in the Panabako with
the upper unit forming 'sugarloaf' cappings above the lower sandstones. These structures are characteristic of high energy
environments (Ayite et al., 2008) and may also be remnants of the Sturtian glaciation reworked by some marine or fluvial
375   activities.

3.5 Hydrogeological applications of the Geological Model

The 3D geological model developed in this research is to be used as the basis for conceptualizing the hydrogeological context of the basin and the larger Voltaian Supergroup. For instance, the apparent detection of the valleys within the Panabako formation may provide an indication of a deeper, prolific aquifer system which has not been noted before in the hydrogeology of the Voltaian Supergroup. The presence of such systems in the Voltaian would have significant implications for the large scale development of groundwater resources for irrigation and other income generation ventures in the area. The Voltaian Supergroup has been noted as a difficult terrain in terms of groundwater resources development and the Nasia Basin, in particular, is one of the basins where high borehole failure rates have led to chronic domestic water access challenges over several years. Within or after the current DANIDA project, the paleovalleys need to be further investigated, leading to both seismic investigations and the drilling of much deeper boreholes penetrating them.

3.6 Conclusion

The present research investigates the concrete possibility of using pre-existing airborne electromagnetic data, originally collected for mineral exploration, to build accurate 3D geological models for hydrogeological purposes. The use of this specific kind of data (B-field time-domain electromagnetic measurements) for this scope is quite novel per se and, in this specific case, allowed the reconstruction of the stratigraphy of the Nasia basin within the Voltaian sedimentary basin. In particular, the proposed geomodelling strategy made possible to infer the presence of paleochannels that have been identified as being pre-Marinoan and may be products of a glaciation event within the Sturtian (old-Cryogenian). The valleys correlate with glacial deposits observed in the Wassangara group of the Taoudeni basin. This group is found within the Supergroup 1, which correlates with the Bombouaka rocks of the Voltaian basin. Together, the paleovalleys and the glacial deposits give further evidence for a snowball earth event that possibly covered the entire Earth during the Neoproterozoic. So, the impact of these finding goes beyond the discover of potential groundwater reservoirs (by itself , extremely relevant from a socio-economic perspective) and can contribute to a rethinking of the stratigraphy of the region and confirm the Neoproterozoic Snowball Earth hypothesis.

Author Contribution

Elikplim Abla Dzikunoo: Investigation, Data Curation, Methodology, Visualization, Writing – original draft, Writing – review & editing;

Giulio Vignoli: Conceptualization, Funding Acquisition, Investigation, Data Curation, Methodology, Software & Algorithm development, Supervision, Validation, Writing – review & editing;

Flemming Jørgensen: Investigation, Methodology, Supervision, Validation, Writing – review & editing;

410 **Sandow Mark Yidana**: Conceptualization, Funding Acquisition, Project Administration, Supervision, Validation, Writing – review & editing;

Bruce Banoeng-Yakubo: Supervision.

Acknowledgments

415 The authors would like to thank DANIDA for its support to this research through the South-driven project: "Ground Water Development and Sustainable Agriculture (Proj. Code: 14-P02-GHA)", also known as "GhanAqua"; and the Geological Survey Authority of Ghana for providing most of the data and for its invaluable help. In this respect, a special thank goes to Mr. Mensah and the director, Dr. Duodu. In addition, the authors are very grateful to Kurt Klitten and Per Kalvig from the Geological Survey of Denmark and Greenland for their love for Ghana and for making this adventure possible.

420 **References**

Asch, T., Abraham, J., & Irons, T.: A Discussion on Depth of Investigation in Geophysics and AEM Inversion Results, SEG Technical Program Expanded Abstracts 2015, 2072-2076, https://doi.org/10.1190/segam2015-5915199.1, 2015.

Anani, C. Y., Mahamuda, A., Kwayisi, D., &Asiedu, D. K.: Provenance of sandstones from the NeoproterozoicBombouaka Group of the Volta Basin, northeasten Ghana, Arab J Geosci., 10, 465, doi: 10.1007/s12517-017-3243-2, 2017.

425 Auken, E., Christiansen, A. V., Kirkegaard, C., Fiandaca, G., Schamper, C., Behroozmand, A. A., Binley, A., Nielsen, E., Effersø, F., Christensen, N. B., Sørensen, K., Foged, N., & Vignoli, G.: An overview of a highly versatile forward and stable inverse algorithm for airborne, ground-based and borehole electromagnetic and electric data, Exploration Geophysics, 46, 223-235, doi:10.1071/EG13097, 2014.

Ayite, A., Awua, F., & Kalvig, P.: Lithostratigraphy of the Gambaga Massif, The Voltaian Basin, Ghana, Workshop and 430 Excursion, March 10-17, 2008, 41-44, 2008.

Bechstädt, T., Jäger, H., Rittersbacher, A., Schweisfurth, B., Spence, G., Werner, G. & Boni, M.: The Cryogenian Ghaub Formation of Namibia–new insights into Neoproterozoic glaciations, Earth-science reviews, 177, doi: 10.1016/j.earscirev.2017.11.028, 678-714, 2018.

Bernard, J.: Short note on the depth of investigation of electrical methods. Orléans, Fracia: IRIS Instruments, 8, 2003.

435   Carney, J. N., Jordan, C. J., Thomas, C. W., Condon, D. J., Kemp, S. J., & Duodo, J. A.: Lithostratigraphy, sedimentation and evolution of the Volta Basin in Ghana. Precambrian Research, 183, 701-724, doi:10.1016/j.precamres.2010.08.012, 2010.

Christiansen, A. V., & Auken, E.: A global measure for depth of investigation, Geophysics, 77(4), WB171-WB177, doi: 10.4133/1.3614254, 2012.

440   Crowe, W. A., & Jackson-Hicks, S.: Intrabasin deformation of the Volta Basin, The Voltaian Basin, Ghana Workshop and Excursion, March 10 - 17, 2008, 31 - 38, 2008.

Deynoux, M., Affaton, P., Trompette, R., & Villeneuve, M.: Pan-African tectonic evolution and glacial events registered in Neoproterozoic to Cambrian cratonic and foreland basins of West Africa. *Journal of African Earth Sciences*, *46*(5), pp.397-426, 2006.

445   Dzikunoo, E., Jørgensen, F., Vignoli, G., Banoeng-Yakubo, B., & Yidana, S. M.: A 3D geological model of the Nasia sub-basin, Northern Ghana - Interpretations from the inversion results of reprocessed GEOTEM data, AEM 2018 / 7th International Workshop on Airborne Electromagnetics Kolding - Denmark, June 17-20, 2018, Abstract 52, 2018.

Eguavoen, I.: The political ecology of household water in Northern Ghana, LIT VerlagMünster, 10, 2008.

FAO: Socio-Economic and Ecological Characteristics. http://www.fao.org/docrep/004/ab388e/ab388e02.htm, last access: 07
450   October 2019.

Fugro Airborne Surveys: Logistics and Processing Report, Airborne Magnetic and GEOTEM Survey, Areas 1 to 8, Ghana, 92, 2009a.

Fugro Airborne Surveys Interpretation: Airborne Geophysical Survey over the Volta River Basin and Keta Basin Geological Interpretation Summary Report, FCR2350/Job No. 1769, 2009b.

455   Gaisie, J. S., & Winter, J.: Tillite in the Togo formation in Ghana. Accra, Ghana, 1973.

Geological Survey Department, British Geological Survey; Fugro Airborne Surveys Limited: Radiometric Regolith-landform Interpretation SHEET 1002/1001/100, Mining Sector Support Programme: Project Number 8ACP GH 027/13, 2006.

Goddéris, Y., Donnadieu, Y., Nédélac, A., Dupré, B., Dessert, C., Grard, A., Ramstein, G., François, L. M.: The Sturtian
460 'snowball' glaciation: fire and ice, Earth and Planetry Science Letters, 211, doi: 10.1016/S0012-821X(03)00197-3, 1-12,
2003

Gulbrandsen, M. L., Jørgensen, F., Dahlqvist, P., & Persson, L.: A 3D geological soil-modelling workflow using AEM data -
A case study from Gotland, Sweden. 7th International Workshop on Airborne Electromagnetics, Kolding - Denmark, June
17 - 20, p. 4.,2018.

465 Hoffman, P.F. & Schrag, D.P.: The snowball Earth hypothesis: testing the limits of global change. *Terra nova*, *14*(3),
pp.129-155, 2002.

Hoffman, P.F. & Li, Z.X.: A palaeogeographic context for Neoproterozoic glaciation, Palaeogeography, Palaeoclimatology,
Palaeoecology, 277(3-4), doi:10.1016/j.palaeo.2009.03.013,158-172, 2009.

Høyer, A.-S., Jørgensen, F., Foged, N., He, X., & Christiansen, A. V.: Three-dimensional geological modelling of AEM
470 resistivity data - A comparison of three methods, Journal of Applied Geophysics, 65-78, doi: 10.1016/j.jappgeo.2015.02.005,
2015.

Høyer, A. S., Vignoli, G., Hansen, T. M., Keefer, D. A., &Jørgensen, F.: Multiple-point statistical simulation for
hydrogeological models: 3-D training image development and conditioning strategies, Hydrology and Earth System
Sciences, 21(12), doi: 10.5194/hess-21-6069-2017, 6069, 2017.

475 Jessell, M., Boamah, K., Duodu, J. A., & Ley-Cooper, Y.: Geophysical evidence for a major palaeochannel within the
Obosum Group of the Volta Basin, Northern Region, Ghana, Journal of African Earth Sciences, 112, 586-596,
doi:10.1016/j.jafrearsci.2015.04.007, 2015.

Jordan, C. J., Carney, J. N., Thomas, C. W., McDonnell, P., Turner, P., McManus, K., &McEvoy, F. M.: Ghana Airborne
Geophysics Project: BGS Final Report, British Geological Survey Commissioned Report, CR/09/02, 2009.

480 Jørgensen, F., Møller, R. R., Lars, N., Jensen, N.-P., Christiansen, A. V., &Sandersen, P. B.: A method for cognitive 3D
geological voxel modelling of AEM data, Bulletin of Engineering Geology and the Environment, 72(3 - 4), 421-432,
doi:10.1007/s10064-013-0487-2, 2013.

Jørgensen, F., Høyer, A.-S., Sandersen, P. B., He, X., &Foged, N.: Combining 3D geological modelling techniques to
address variations in geology, data type and density - An example from Southern Denmark, Computers & Geosciences, 81,
485 53-63, doi:10.1016/j.cageo.2015.04.010, 2015.

Jørgensen, F., Menghini, A., Vignoli, G., Viezzoli, A., Salas, C., Best, M. E., & Pedersen, S. A.: Structural Geology Interpreted from AEM Data-Folded Terrain at the Foothills of Rocky Mountains, British Columbia, 2nd European Airborne Electromagnetics Conference. Malmö, Sweden, September 3 - 7, 2017.

Jørgensen, F., & Sandersen, P. B.: Buried and open tunnel valleys in Denmark - erosion beneath multiple ice sheets,
490   Quaternary Science Reviews, 25, 1339 - 1363, doi: 10.1016/j.quascirev.2005.11.006, 2006.

Kalsbeek, F., Frei, D., &Affaton, P.: Constraints on provenance, stratigraphic correlation and structural context of the Volta basin, Ghana, from detrital zircon geochronology: An Amazonian connection? Sedimentary Geology, 86-95, doi: 10.1016/j.sedgeo.2008.10.005, 2008.

Kehew, A. E., Piotrowski, J. A., &Jørgensen, F.: Tunnel valleys: Concepts and controversies - A review, Earth Science
495   Review, 113(1 - 2), 33 - 58, doi: 10.1016/j.earscirev.2012.02.002, 2012.

Ley-Cooper, A. Y., Viezzoli, A., Guillemoteau, J., Vignoli , G., Macnae, J., Cox, L., &Munday, T.: Airborne electromagnetic modelling options and their consequences in target definition, Exploration Geophysics, 46, 74-84, doi: 10.1071/eg14045, 2014.

Loke, M. H., & Barker, R. D.: Rapid least-squares inversion of apparent resistivity pseudosections by a quasi-Newton
500   method 1, Geophysical prospecting, 44(1), 131-152, doi: 10.1111/j.1365-2478.1996.tb00142.x, 1996.

Loke, M. H.: Rapid 2D resistivity and Iinversion using the least-squares method RES2DINV. Program Manual, 1997.

MacGabhann, B.A.: Age constraints on Precambrian glaciations and the subdivision of Neoproterozoic time, IUGS EdiacaranSubcommission Circular, August 21, 2005.

Meier, P., Kalscheuer, T., Podgorskii, J. E., Kgotlhang, L., Green, A. G., Greenhalgh, S., Rabenstein, L., Doetsch, J.,
505   Kinzelbach, W., Auken, E., Mikkelsen, P., Foged, N., Jaba, B.G., Tshoso, G., &Ntibinyane, O.: Hydrogeophysical investigations in the western and north-central Okavango Delta (Botswana) based on helicopter and ground-based transient electromagnetic data and electrical resistance tomography, Geophysics, 79(5), B201-B211, doi: 10.1190/geo2014-0001.1, 2014.

Oldenborger, G. A., Logan, C. E., Hinton, M. J., Sapia , V., Pugin, A. J., Sharpe, D. R., Calderhead, A. I., & Russell, H. A.:
510   3D Hydrogeological Model Building Using Airborne Electromagnetic Data, Near Surface Geoscience 2014-20th European Meeting of Environmental and Engineering Geophysics, Athens - Greece,September, 14 - 18, 2014.

Pryet, A., Ramm, J., Chiles, J.-P., &Auken, E.: 3D resistivity gridding of large AEM datasets: A step tworad enhanced geological interpretation. Journal of Applied Geophysics, no. 2, 277-283, 2011.

Rapiti, A., Jørgensen, F., Menghini, A., Viezzoli, A., &Vignoli, G.: Geological Modelling Implications-Different Inversion Strategies from AEM Data, 24th European Meeting of Environmental and Engineering Geophysics, Porto - Portugal, doi: 10.3997/2214-4609.201802508, 2018.

Ross, M., Parent, M., & Lefebvre, R.: 3D geologic framework models for regional hydrogeology and land-use management: a case study from a Quaternary basin of southwestern Quebec, Canada. Hydrogeology Journal, 13(5-6), 690-707. Doi:10.1007/s10040-004-0365-x, 2005.

Sapia, V., Oldenborger, G. A., Jørgensen, F., Pugin, A. J.-M., Marchetti, M., &Viezzoli, A.: 3D modeling of buried valley geology using airborne electromagnetic data. Interpretation, 3(4), SAC9-SAC22, 2015.

Shields-Zhou, G. A., Deynoux, M., &Och, L.: Chapter 11 The record of Neoproterozoic glaciation in the Taoudéni Basin, NW Africa. Geological Society, London, Memoirs, 36(1), 163–171. https://doi.org/10.1144/m36.11, 2011.

Smith, R., & Annan, P.: The use of B-field measurements in airborne time-domain system: Part I. Benefits of B-field versus dB/dt data. Exploration Geophysics, 24-29, 1998.

Tarantola, A.: Popper, Bayes and the inverse problem. Nature physics, 2(8), 492, https://doi.org/10.1038/nphys375,2006.

Turner, A. K.: Challenges and trends for geological modelling and visualisation. Bulletin of Engineering Geology and the Environment, 65, 109-127. doi:10.1007/s10064-005-0015-0, 2006.

Van der Vegt, P., Janszen, A., &Moscariello, A.: Tunnel Valleys: Current Knowledge and Future Perspectives. Geological Society, London, Special Publications, 368(1), 75-97, doi: 10.1144/sp368.13, 2012.

Viezzoli, A., Christiansen, A. V., Auken, E., &Sørensen, K.: Quasi-3D modeling of airborne TEM data by spatially constrained inversion. Geophysics, 73(3), F105-F113, https://doi.org/10.1190/1.2895521, 2008.

Viezzoli, A., Munday, T.,Auken, E.,& Christiansen, A.V.: Accurate quasi 3D versus practical full 3D inversion of AEM data–the Bookpurnong case study. Preview, 149, 23-31, https://doi.org/10.1071/PVv2010n149p23, 2010.

Viezzoli, A., Jørgensen, F., &Sørensen, C.:Flawed processing of airborne EM data affecting hydrogeological interpretation. Groundwater, 51(2), 191-202, https://doi.org/10.1111/j.1745-6584.2012.00958.x, 2013.

Vignoli, G., Cassiani, G., Rossi, M., Deiana, R., Boaga, J., &Fabbri, P.: Geophysical characterization of a small pre-Alpine catchment, Journal of Applied Geophysics, 80, 32-42, https://doi.org/10.1016/j.jappgeo.2012.01.007, 2012.

Vignoli, G., Fiandaca, G., Christiansen, A. V., Kirkegaard, C., &Auken, E.: Sharp spatially constrained inversion with 540 applications to transient electromagnetic data. Geophysical Prospecting, 63(1), 243-255, doi: 10.1111/1365-2478.12185, 2015.

Vignoli, G., Sapia, V., Menghini, A., &Viezzoli, A.: Examples of improved inversion of different airborne electromagnetic datasets via sharp regularization. Journal of Environmental and Engineering Geophysics, 22(1), 51-61, doi: 10.2113/JEEG22.1.51, 2017.

545 Villeneuve, M., &Cornée, J. J.:Structure, evolution and palaeogeography of the West African craton and bordering belts during the Neoproterozoic.In Precambrian Research (Vol. 69, pp. 307–326). https://doi.org/10.1016/0301-9268(94)90094-9, 1994.
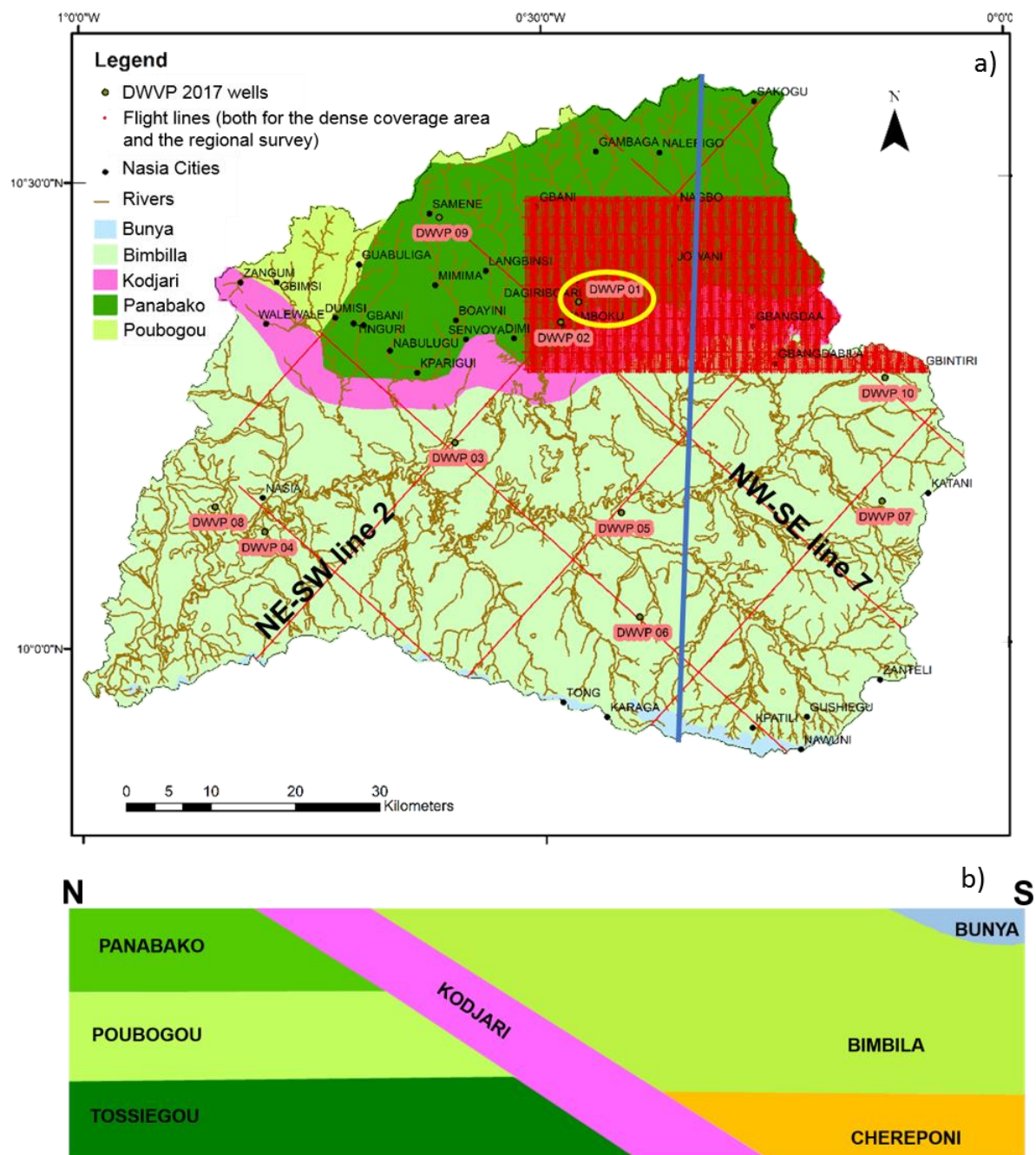
Figure 1: (a) Geologic Map of Nasia sub-basin after Carney et. al (2010); (b) Conceptual Model of the geology along a cross sectional N-S line within the study area (solid blue line in the panel a).
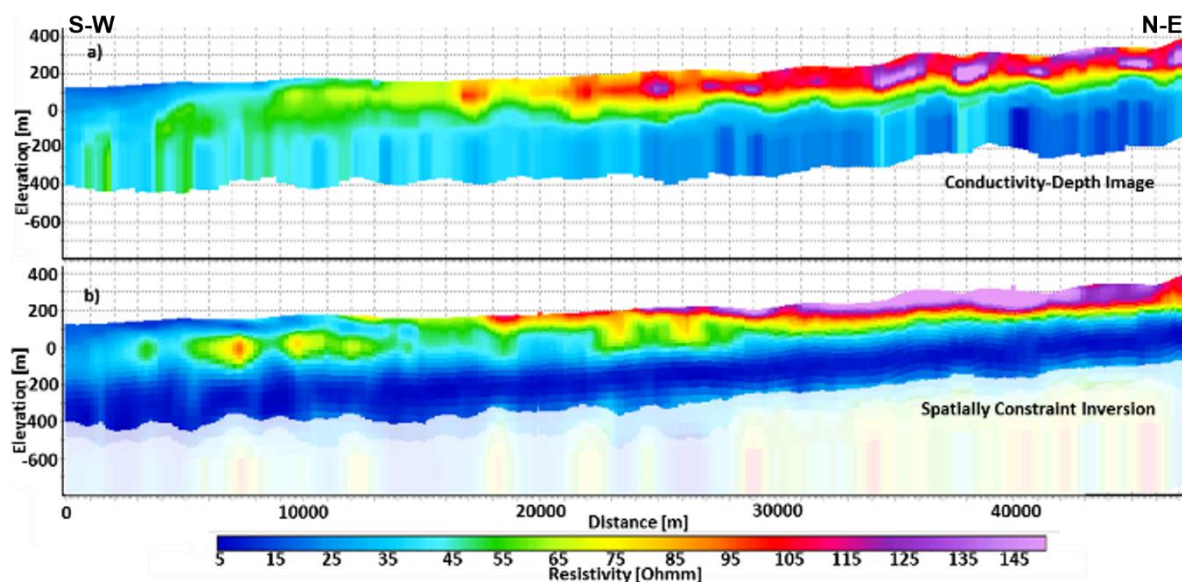
Figure 2. (a) The original Conductivity-Depth Image (CDI) along NE-SW line 2 (Fig. 1a); (b) the associated result obtained with the new data processing and inversion approach (smooth Spatially Constrained Inversion).
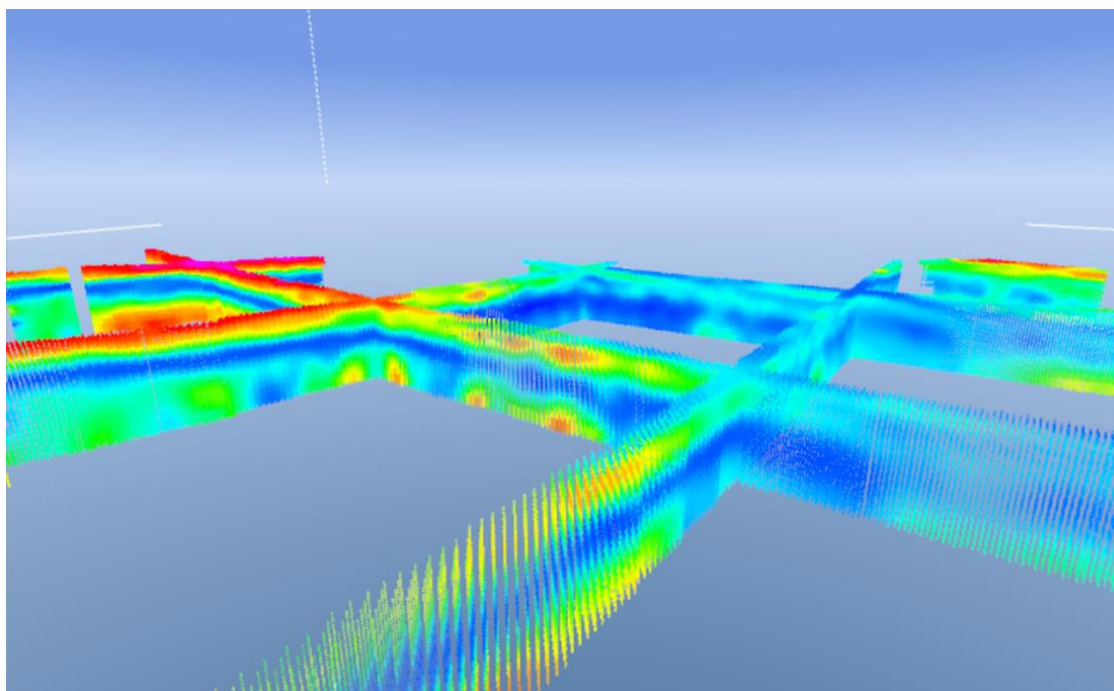
555

Figure 3. A 3D view of the B-field SCI results along the 20km x 20km grid lines in the study area. These soundings were used as basis for geologic interpretation and modelling.
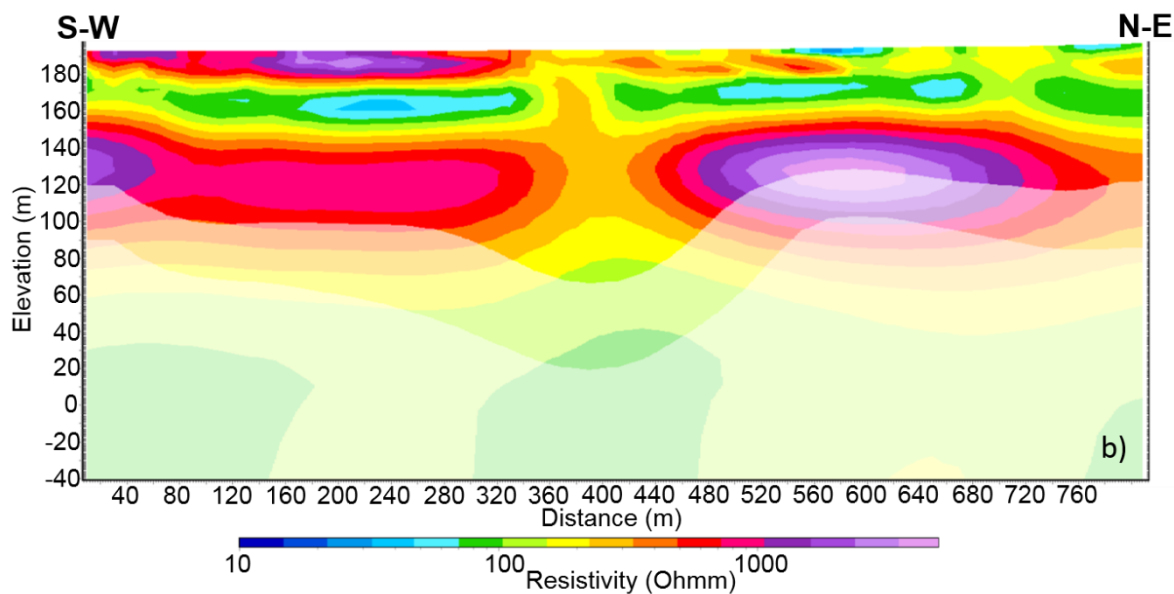
560 **Figure 4. Results of the ERT performed preliminarily to the drilling of the DWVP 01 well (the location of the midpoint of the line is shown in Fig.1a, highlighted by a yellow circle). The sensitivity of the data with respect to the model parameter values reduces significantly below the depth of investigation (DOI – Asch et al., 2015) that is indicated by the white overlay.**
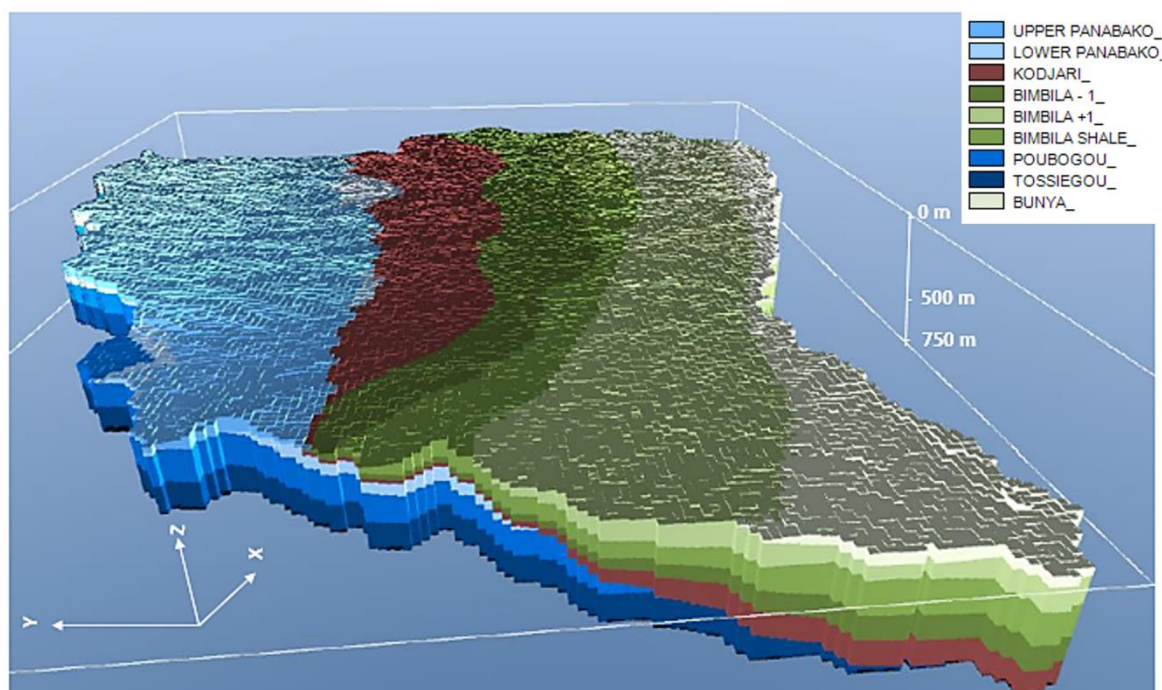
565

Figure 5. 3D geological model of the Nasia sub-basin resulting from the combined interpretation of the B-field airborne data, the prior geological knowledge of the area, and the available wells.

570
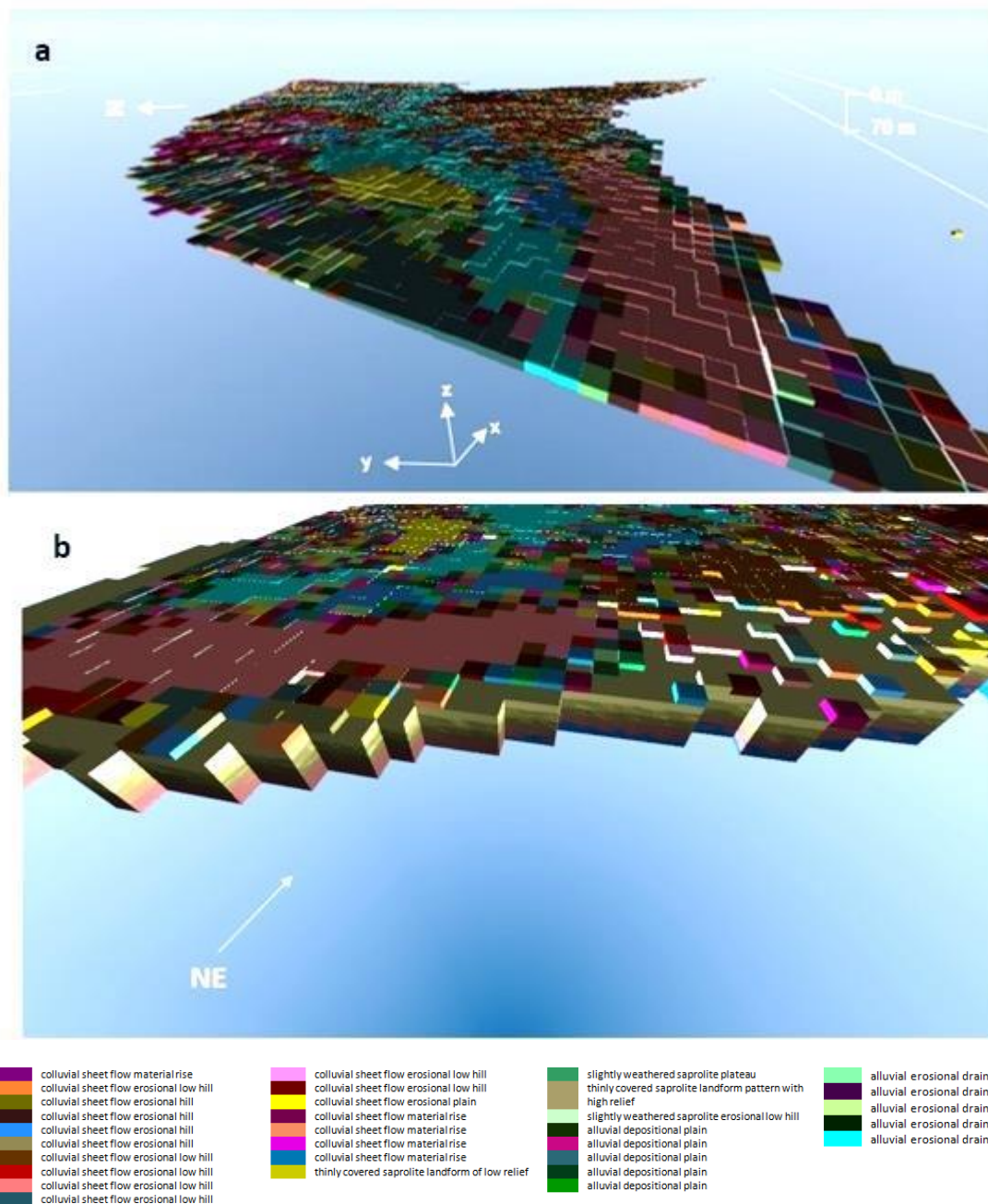
Figure 6. (a) 3D model of the regolith volume in the study area. (b) 3D model of a combined bedrock and regolith model
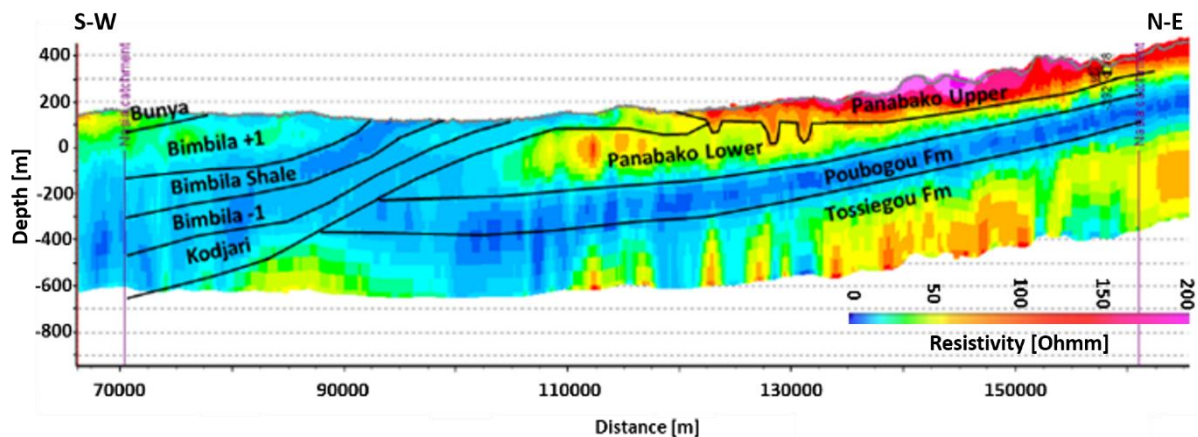
Figure 7. Cross-section from the North along NE-SW line 2 of the study area (see Fig.1a for the location) with conceptual geological interpretations showing U-shaped valleys (between 120 and 130 km).
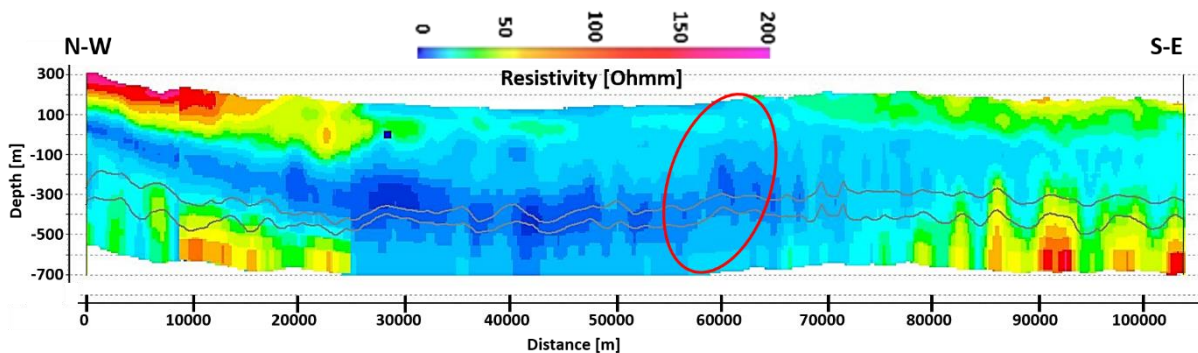
Figure 8. Cross-section along NW-SE line 7 (Fig. 1a) showing faulting (within the red circle) in the Bimbila. The DOI is showed as a solid grey line (there are two of them accordingly to their definition – more details on this distinction can be found in Christiansen and Auken, 2012).